Sensitivity studies on power transformer ferroresonance of a 400 kV double circuit

C. Charalambous, Z.D. Wang, M. Osborne and P. Jarman

Abstract: The ability to predict ferroresonance significantly relies on the accuracy of the transformer model and the power system's parameters. The accomplishment of a suitable simulation model allows the sensitivity studies to be performed to determine the degree of influence of various components and parameters of the ferroresonance phenomenon such as line length, point-on-wave switching and transformer core loss. The modelling work carried out in ATP (commercially available software) on a 1000 MV A 400/275/13 kV power transformer model is described and the simulation with field ferroresonance test recordings is verified. The maps that define the boundaries between safe and ferroresonant (fundamental, subharmonic, chaotic) regions as a function of system parameters are created through the sensitivity studies performed.

1 Introduction

Certain circuit configurations of the UK transmission network provide an ideal environment for ferroresonance to occur. The possibility of the occurrence of ferroresonance can be eliminated by the use of additional circuit breakers; however, the economic justification needs to be carefully considered. One characteristic example of power transformer ferroresonance is although one side of a double-circuit transmission line connected to a transformer is switched out it remains energised because of being capacitively coupled with the other live parallel circuit. Recovering from this condition requires the operation of a disconnector or earth switch in the resonating circuit, potentially resulting in arcing and damage, or switching the parallel circuit resulting in an unplanned double-circuit outage.

The UK experience, for the power transformer case, suggests that one in ten circuit de-energisations can be driven into ferroresonance, the probability depending upon the appropriate initial conditions being established [1]. The initiation of ferroresonance that is defined as stochastic or in some cases chaotic depends on various system and plant parameters [2]. When a ferroresonance occurs, typically a non-sinusoidal (peaky) current of around 50–100 A_{rms}, 200–350 A_{peak}, is generated at fundamental frequency (50 Hz) or at its subharmonics (e.g. $16^{2/3}$ Hz). Failing to detect or remove a ferroresonant condition can result in overheating of parts of the transformer because it is being repeatedly driven into saturation.

This paper builds on previous work which describes the modelling carried out to reproduce the field ferroresonance recordings obtained by National Grid on a 37 km circuit configuration which was known to exhibit ferroresonance [3]. The analysis further investigates the influence of a number of system and plant parameters on ferroresonance through sensitivity studies.

The sensitivity studies performed concentrate on interactions such as (i) point-on-wave (POW) switching and transmission line length and (ii) core losses and POW. The effect of these system parameters on the energy dissipated within the transformer during ferroresonance, on the magnitude of ferroresonant voltage and current is deduced. Moreover, the simulation results allow the creation of maps that define the boundaries between safe and ferroresonant (fundamental, subharmonic, chaotic) regions as a function of system parameters.

2 Model description

2.1 400 kV double-circuit configuration

The testing was carried out on the 400 kV circuit which was identified as a suitable circuit that could be induced to resonate. The purpose of the tests was to establish the likelihood of the occurrence of ferroresonance on SGT 1 shown in Fig. 1 and the impact on the disconnector switch during quenching of the resonant condition [4]. Fig. 1 illustrates a single line diagram of the Brinsworth/Thorpe Marsh circuit arrangement. The length of the parallel overhead line circuit is ~37 km and the feeder has a 1000 MV A 400/275/13 kV power transformer. It should be noted that this is not a normal running arrangement; however, to facilitate the testing, this configuration was used on the day.

The field recordings have been obtained by applying POW switching on the circuit, utilising a circuit breaker. The circuit breaker was tripped via an external POW control device to induce ferroresonance. After each switching operation, the POW switching control was advanced by 1 ms until fundamental and subharmonic mode ferroresonances were established. This type of switching prevents switching over-voltage conditions and provides a degree of controllability to the tests.

2.2 Simulation model

During the past decade, a number of studies have been carried out to evaluate the performance of a transformer

doi:10.1049/iet-gtd:20070141

Paper first received 3rd April and in revised form 19th July 2007

C. Charalambous and Z.D. Wang are with the School of Electrical and Electronic Engineering, The University of Manchester, Manchester M60 1QD, UK

M. Osborne and P. Jarman are with National Grid, UK

E-mail: Charalambos.charalambous@manchester.ac.uk

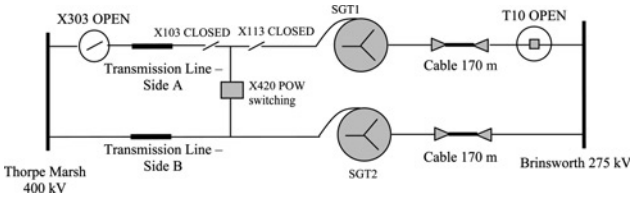

Fig. 1 *Single line diagram of the Brinsworth/Thorpe Marsh circuit arrangement*

model under ferroresonance. Quite a few studies have proposed mathematical models and several others have published results based on computer simulation models. A comprehensive overview of the ferroresonance phenomenon with the associated computer simulation models is given in [5]. Table 1 illustrates a summarised version of some characteristic nonlinear transformer models that have been proposed in the related literature, along with their capabilities in incorporating modelling features such as saturation, hysteresis and so on.

For the purpose of this study, an ATP-based model has been developed [3] to simulate the testing carried out on the circuit with the ultimate purpose to match field test recordings that were available. The transformer has been modelled utilising the BCTRAN module of ATP draw [12]. Fig. 2 illustrates a layout of the simulation model, which includes a description of the components of the model.

The main components of the network are a parallel overhead line circuit and a 1000 MVA 400/275/13 kV

Table 1: Description of transformer simulation models

References	Model capabilities			
	Saturation effect	Hysteresis losses	Eddy current losses	Anomalous losses
[6]	√[a]	√	√	
[7]	√	√	√	
[8]	√			
[9]	√	√	√	
[10]	√[a]			
[11]	√[a]	√	√	√

[a]Individual core section is modelled separately

transformer. The line is 37-km long and is modelled using the typical overhead line spacings for a 400 kV double circuit [13]. The transmission line has been modelled in ATP on a Bergeron model (constant parameter KCLee or Clark models) [12]. The transformer has a five-limb core, and the percentage ratio of the yoke and the side limbs is 60% of the main limb. It was manufactured in 1996 and there are no bolts used in the core and yoke. The elements of the transformer matrices are derived from standard open and short circuit tests obtained by the manufacturer. The data used in this simulation model include impedances and losses averaged from the test results of eight transformers and these are tabulated in Table 2. With a low-frequency phenomenon such as ferroresonance, saturation effects must be considered. These transformers have been modelled by attaching the nonlinear characteristics externally in the form of a nonlinear inductive element branch.

It should be noted that the impedances and load losses can only be measured for winding pairs, but the designed load capability for the tertiary winding of this 1000 MV A design is only 60 MV A compared with the 1000 MV A throughput for the HV and LV terminals. Thus the H-T and L-T losses and impedances were measured at 60 MV A. For this simulation model, a common base load is chosen to be 1000 MV A. A dynamic resistance model for the core losses was achieved within the BCTRAN model. The authors have used the factory test results for the 400/275/13 kV 1000 MV A autotransformer. The available magnetising characteristics are as follows.

The 90% voltage, equivalent to 1.53 T: open-circuit loss 57.2 kW (0.00572% at 1000 MV A base), magnetising current 0.00984% at 1000 MV A base. The 100% voltage, equivalent to 1.7 T: open-circuit loss 74.4 kW (0.00744% at 1000 MV A base), magnetising current 0.01228% at 1000 MV A base. The 110% voltage, equivalent to 1.87 T: open-circuit loss 107.1 kW (0.01071% at 1000 MV A base), magnetising current 0.10163% at 1000 MV A base. The V–I characteristics are automatically produced utilising the factory open-circuit test results and are illustrated in Fig. 3. The average power curve is also illustrated in Fig. 3.

Zero sequence data were not available and therefore the zero sequence data that had been employed in this simulation model has been set equal to the positive sequence data. This is a reasonable assumption to make for a five-limb core transformer with a tertiary winding. Provision

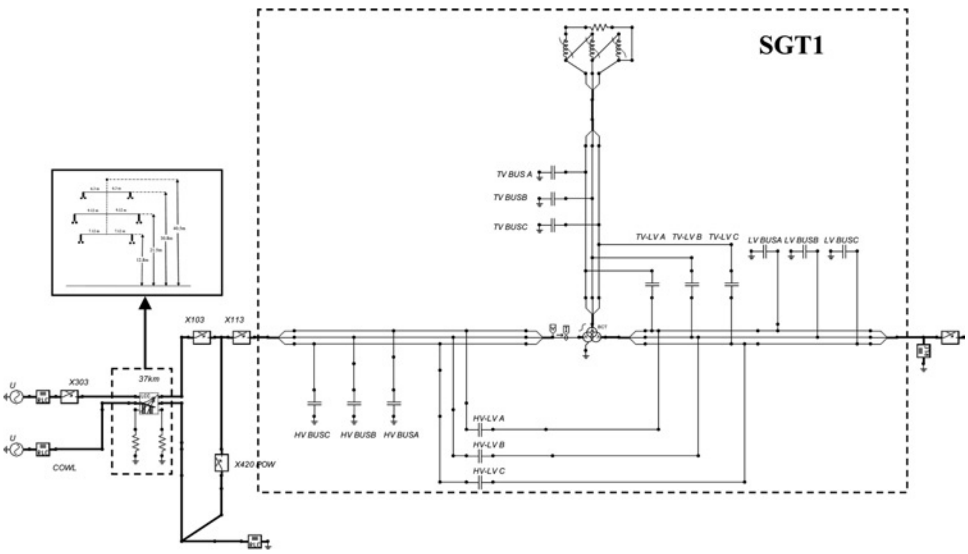

Fig. 2 *Layout of ATPDraw simulation model*

Table 2: Transformer short-circuit factory data

	Impedance, %	Power, MV A	Loss, kW
HV-LV	15.8	1000	1764
HV-TV	117.2 (7.032)	1000 (60)	28677 (1720.62)
LV-TV	91.5 (5.49)	1000 (60)	29875 (1792.5)

of a tertiary winding on five-limb cores drastically alters the zero sequence impedance, since zero sequence currents are able to circulate around the delta tertiary winding and thus balance those flowing into the primary winding [6]. Without a tertiary winding, the five-limb core would have a higher zero sequence impedance because of the fourth and fifth return limbs shunting the high reluctance zero sequence path (air path). The fourth and fifth return limbs of a five-limb core are of much reduced section compared with the three main limbs and a zero sequence test at full load current would cause the fourth and fifth limbs to saturate and the core would turn into a three-limb equivalent. In such a case, the assumption of setting the zero sequence equal to the positive sequence data would not be valid.

Saturation effects, when utilising a BCTRAN model, can be considered by attaching the nonlinear characteristics externally in the form of a nonlinear element branch. Nonlinear inductances can be modelled as two-slope piece-wise linear inductances, with sufficient accuracy [5]. The slope in the saturated region above the knee reflects the air-core inductance which is almost linear and low compared with the slope in the unsaturated region. In addition, the simulation model has been appropriately tested by utilising true nonlinear saturable inductors. A number of simulations have been repeated using smoother approximation for the nonlinear characteristics to compare the results when the two-type slope has been utilised. The produced results show a negligible alteration on regions and boundaries of the maps presented in Section 5. To produce the same result (i.e. mode of ferroresonance), the POW switching was readjusted in a region of $\pm 10\ \mu s$. Fig. 4 illustrates on the same graph the result obtained when utilising the two-type slope magnetising characteristics and the true nonlinear characteristics.

The transformer magnetisation curve has been derived from manufacturer's data available. For core materials used in modern high-voltage power transformers, hysteresis loops are not significant and therefore a single-valued curve was assumed [14]. Literature survey reveals that the magnetisation can effectively be described by a single-value curve or function [8, 14–16].

For cylindrical coil construction, it is assumed that the flux in the winding closest to the core will mostly go through the core, since there would be very little leakage. This winding is usually the tertiary winding, and it is therefore best to connect the nonlinear inductance across the tertiary terminals. Although attaching the nonlinear effect externally is an approximation, it is reasonably accurate for frequencies below 1 kHz [17].

In low-frequency transformer models, it is possible to represent each winding as one element. This does not come at the expense of accuracy. Bearing that in mind, the simulation model comprises the winding series capacitance, the interwinding and shunt capacitance as lumped elements, which have been calculated considering the

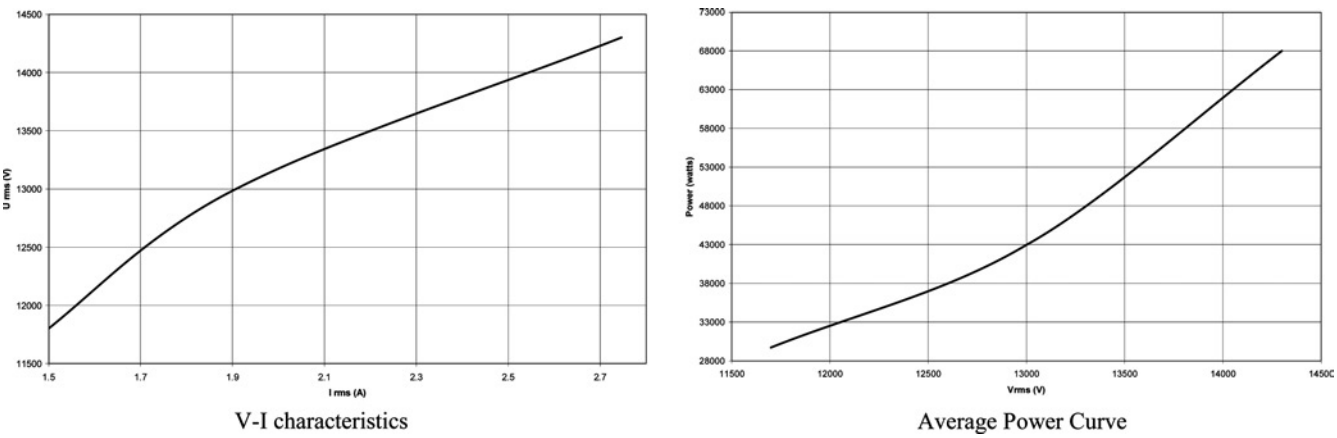

Fig. 3 *V–I characteristics and average power curve*

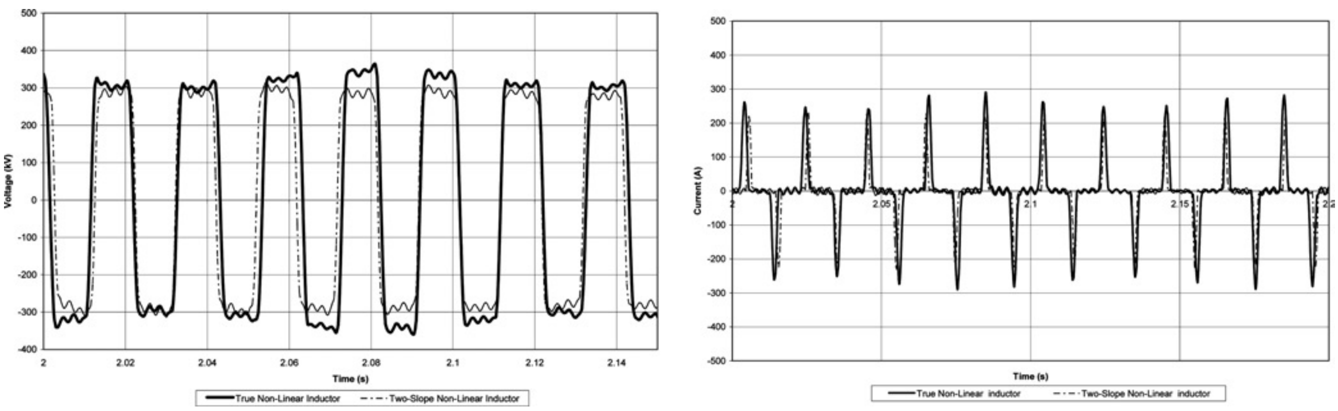

Fig. 4 *Comparison of the true nonlinear and the two-type magnetising characteristics for the fundamental mode produced waveforms*

dimensions, the winding configuration types and the permittivities of the insulation. The methodology applied for the capacitance calculation is presented in [18]. In the case of winding series capacitance calculation, the lumped-element model of [18] calculates the equivalent series capacitance of the winding based on the assumption that the voltage distribution along the turn conductors is linear and the energy stored in the equivalent series capacitance of the winding will be equal to the total energy stored in all the geometric capacitances within the winding.

2.3 Validation of simulation model

Fig. 5 illustrates a comparison of a sector of the final steady-state ferroresonance mode waveforms produced by ATP with those available from field recordings, for the fundamental and subharmonic case, respectively, for just one phase. It should be noted that full-scale validation (in all three phases) of the model has been carried out in [3]. The field test recordings matched with simulation results reasonably well. Consequently, the simulation model can be further utilised to perform sensitivity studies.

It is worth noting that the field test results were obtained by some sort of measurement devices, which have not been modelled in this simulation, as there is no information documented. Furthermore, it is known that field test voltages and currents were captured every 1 ms, where the simulation produces data at every 1 μs. The field test measuring devices proved inefficient to accurately capture the voltage and the current waveforms, especially in the case of the spiky ferroresonant current (Fig. 5*b*). A closer look at the field test ferroresonant current waveform shows a variation in the peak magnitude of the current, whereas the simulation result shows a fairly consistent current magnitude.

3 Sensitivity studies

Literature survey has identified case studies where the series capacitance, the core losses and the source voltage are investigated to determine the effect of these parameters on ferroresonance [2, 14]. The studies were performed using a basic ferroresonant circuit configuration, which was solved by utilising the Ritz method of harmonic balance [19]. Parametric maps are used to assess the effect of the parameters under study, on the location of the borders that define normal and ferroresonant regions.

The sensitivity studies carried out for the scope of this paper utilise the validated simulation model developed. The simulation model provides the authors with the opportunity to assess in detail the degree of influence of the different components and their parameters on the ferroresonance phenomenon. Specifically, the parameters under study are the transmission line length, the POW switching and the core losses.

The transmission line length that feeds the transformer is used to assess the influence of the capacitance on ferroresonance since the line has a line-to-ground capacitance and line-to-line (coupling, or the so-called series in [2, 14]) capacitance. It is more practical to assess transmission line length rather than capacitance values when it comes to optimise circuit configurations (especially of new connections) to ensure system reliability in terms of initiation of ferroresonance. It is reiterated that the ATP-based simulation model reflects on the geometry of the transmission line by considering the typical overhead line spacings for a 400 kV double circuit [13].

The core losses and the POW switching influence the initiation of ferroresonance as will be shown in Section 4. As pointed in [2], the transformer core losses are important and can make a difference between results showing chaotic behaviour, ordinary ferroresonance or normal

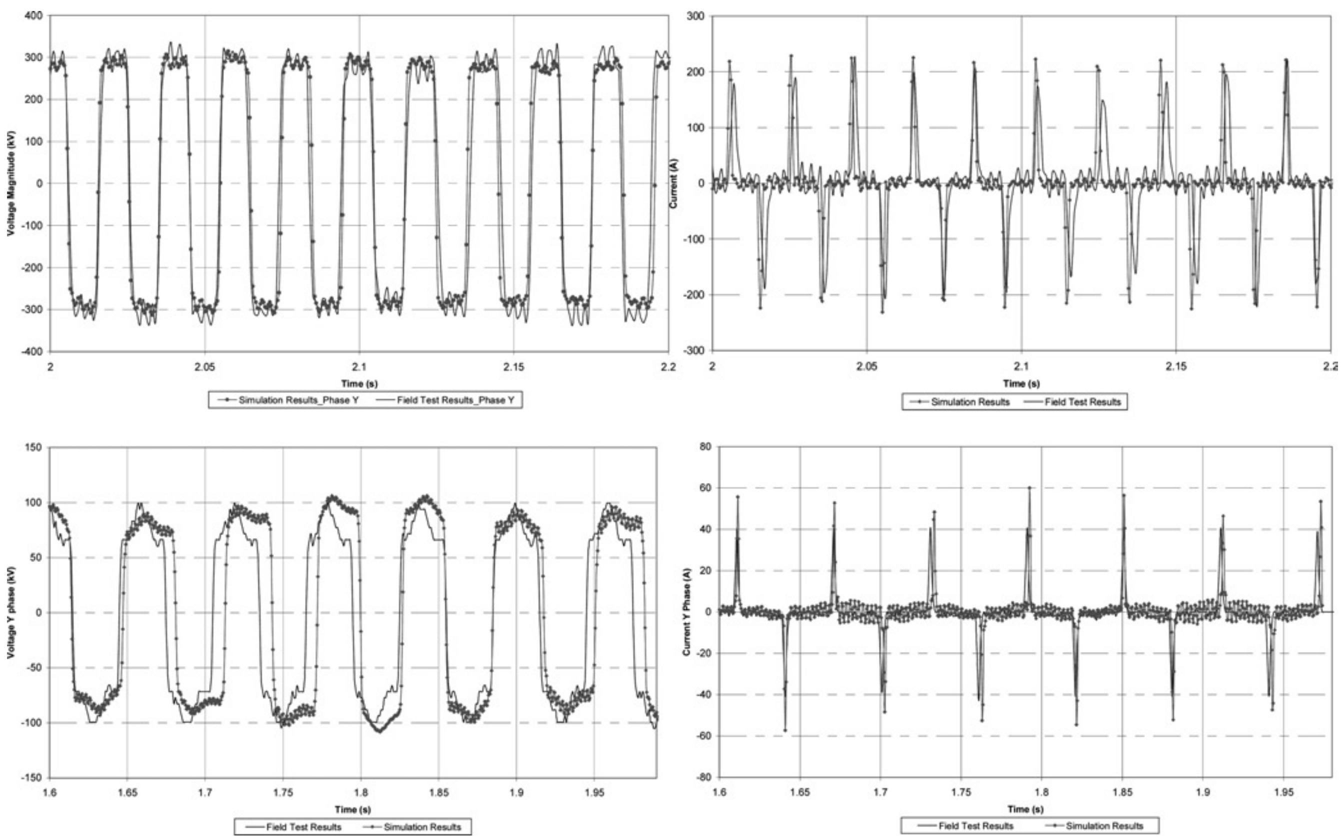

Fig. 5 *Comparison of fundamental and subharmonic mode ferroresonance, section of voltage and current waveform, Y phase*

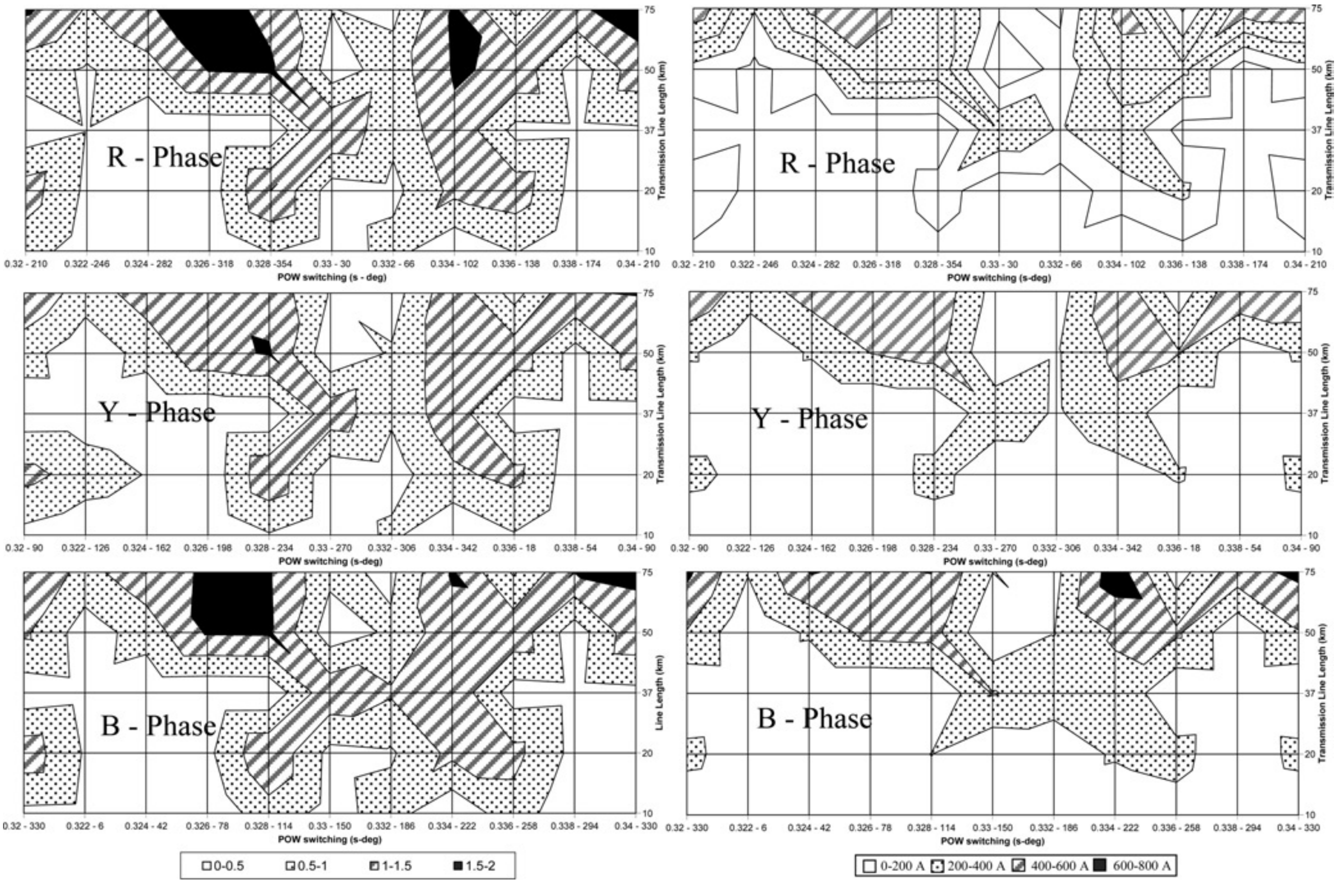

Fig. 6 *Interaction of trans. line length and P.OW: Peak voltage (p.u) and current (A) per phase*

behaviour. Over the last 50 years, transformer core materials have constantly improved, effectively reducing losses. For the scope of this study, the core losses were arbitrarily changed.

The parameters of transmission line length, POW switching and core losses determine their degree of influence on the magnitude of the resulting ferroresonance voltages and currents and the energy supplied to the transformer under ferroresonance conditions, as well as determining the borders between safe and ferroresonant regions.

As far as the energy level is concerned, in the case where ferroresonance does not exceed voltage withstanding levels, it is assumed that the main mechanism for damage to transformers is the heating of magnetic or conducting parts and surrounding insulating materials because of core saturation. By determining the energy (or power) transfer from the system to the transformer under ferroresonance conditions, the amount of energy transferred becomes a useful estimate for potential transformer damage. Undoubtedly, it would need some further consideration of the transformer topology and geometry to determine an accurate energy density distribution.

However, if, for example, the transfer was low, this would have to be very concentrated on a particular part to do any damage, whereas a high value of energy would be a major problem irrespective of where the energy is distributed in the magnetic path during core saturation. It should be noted that the power dissipated through Joule heating will depend on the leakage fields, which is determined during saturation of the core. It is the core leakage flux that will induce current and hence ohmic heating in conducting components. Heat will then be transferred to nearby insulating materials by conduction and convection.

The energy level transferred to the transformer during ferroresonance has been quantified by utilising the expression

$$E = \int_0^t v(t) \times i(t)\,\mathrm{d}t \qquad (1)$$

4 Analysis of results

4.1 Interaction of transmission line length and POW switching

The first case study presents the results obtained from the interaction of transmission line length and POW switching by altering these two parameters and leaving all others unchanged. A series of transmission line lengths have been simulated against a number of POW switching on a complete cycle. The varying transmission line length will

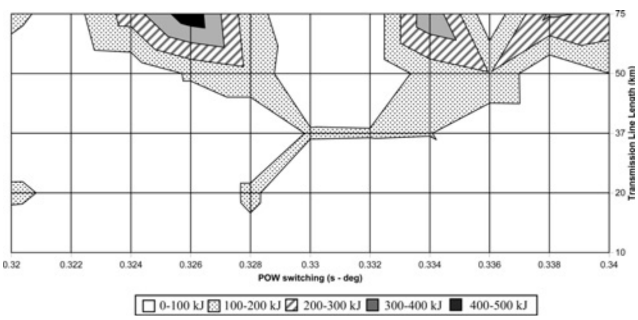

Fig. 7 *Interaction of trans. line length and POW: transformer total energy level*

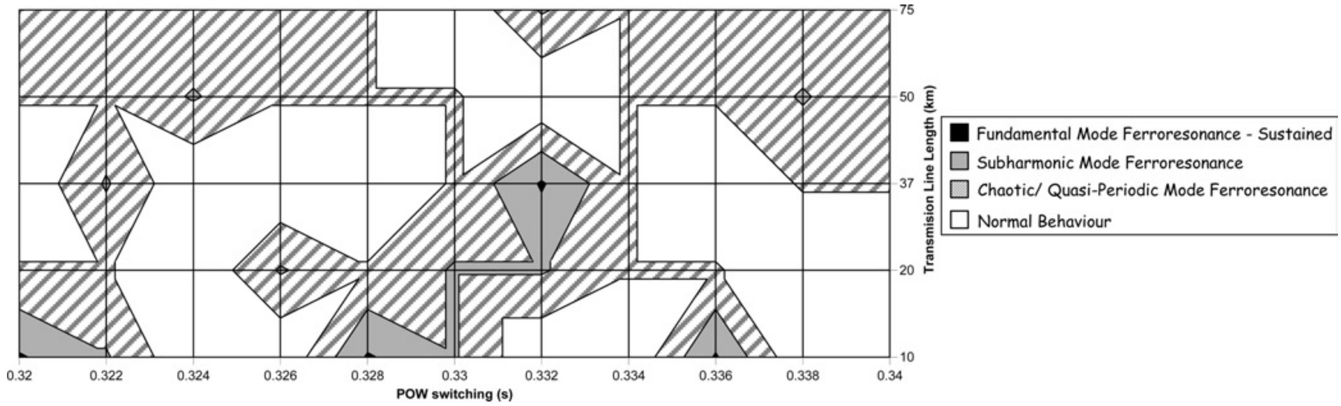

Fig. 8 *Interaction of trans. line length and POW: ferroresonance map*

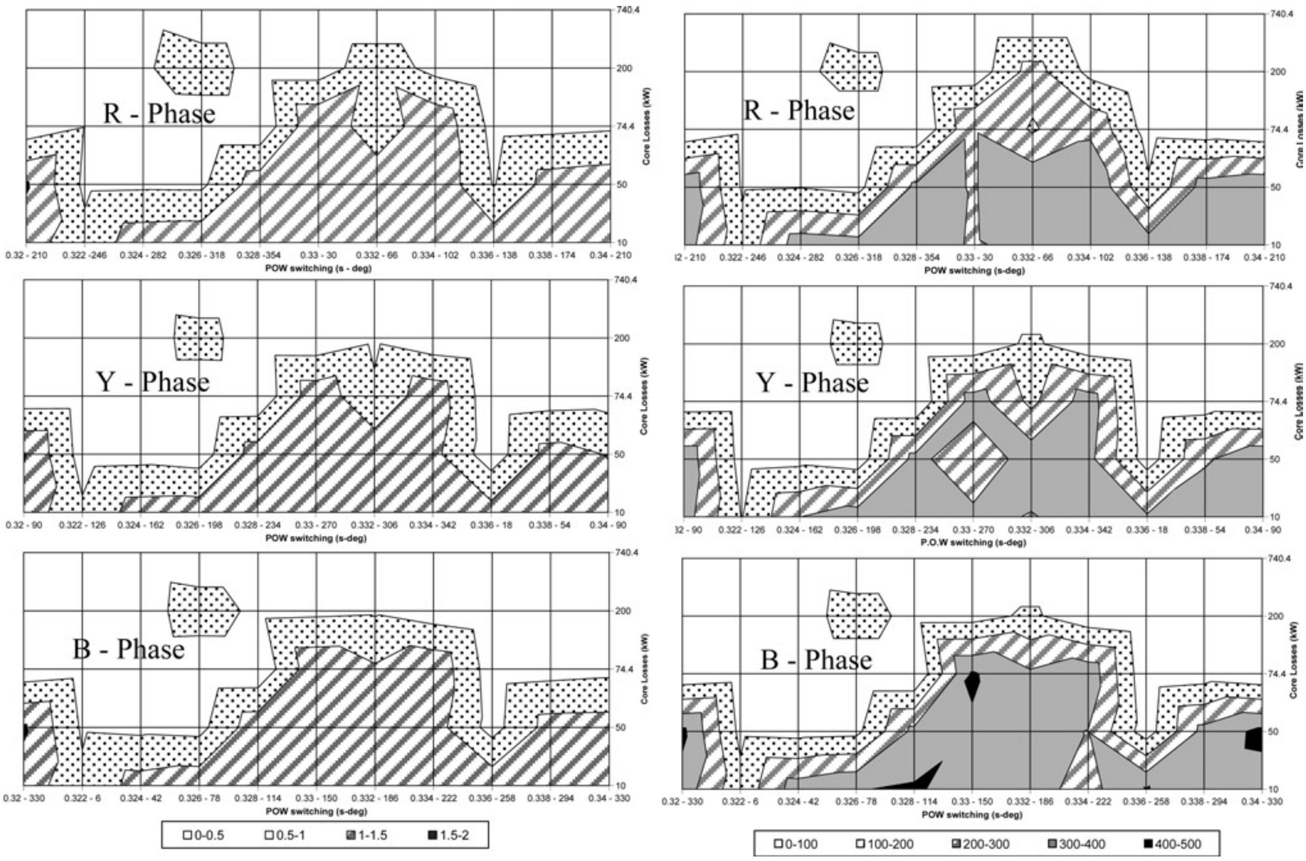

Fig. 9 *Interaction of core losses and P.OW: Peak voltage (p.u) and (A) current per phase*

have an effect on the coupling capacitance through which the isolated transformer is still being energised.

Fig. 6 describes the steady-state (once the transient period ceases to exist) ferroresonant peak voltage values in p.u. and the peak current values for each of the three phases as a function of transmission line length and POW switching. Higher ferroresonant currents and over-voltages (both in magnitude) exist when the feeding transmission line is longer. The magnitude of peak ferroresonant currents lies in the range of 100–500 A. Over-voltages can go up to 2 p.u. and can exist in all three phases. Fig. 6 also illustrates the effect the POW switching has on the magnitude of voltages and currents. There are POW switching times that can maintain current and voltages at low levels even at longer lengths of transmission lines.

Fig. 7 illustrates the energy transfer in the transformer under ferroresonant conditions when considering the interaction of POW switching with the transmission line length. The energy transfer calculation has been performed

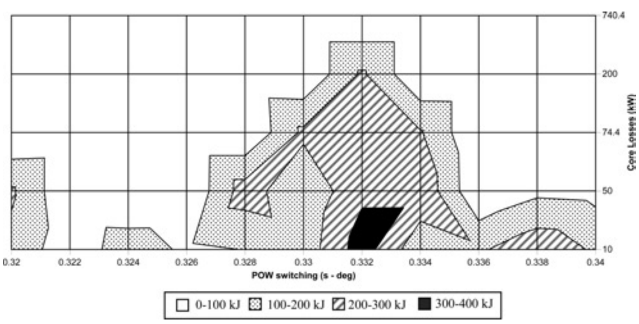

Fig. 10 *Interaction of core losses and POW: transformer total energy level*

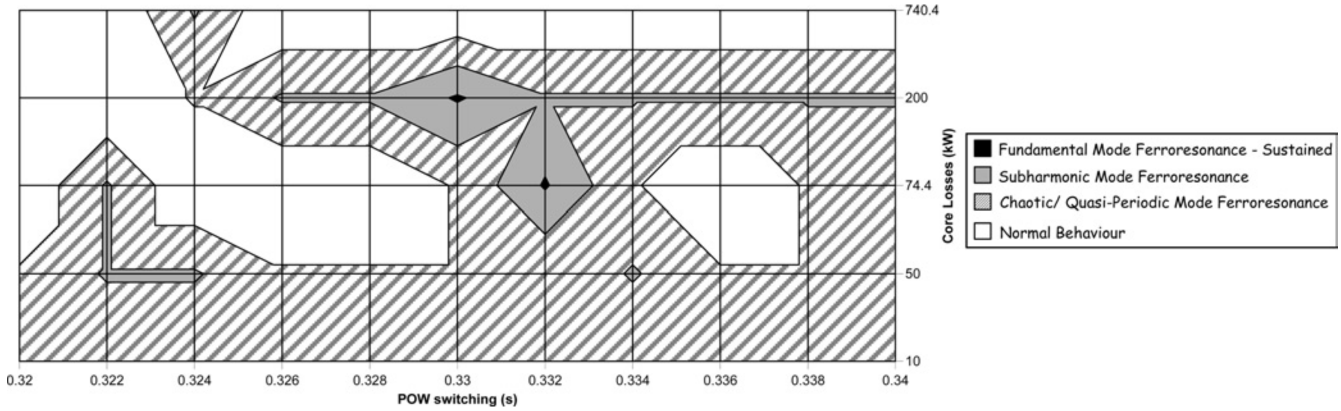

Fig. 11 *Interaction of core losses and POW: ferroresonance map*

at a specific value of core losses (the actual core losses) for 1 s. Because losses are small, ferroresonance will be sustained for quite a long time, unless interrupted. One second of results (excluding the transient period in the cases of fundamental or subharmonic mode ferroresonance) is probably a good projection of the amount of energy per unit time. (Energy values were obtained by integrating voltage and current for a period of 1 second).

The transformer is more susceptible to potential damage from energy transfer under ferroresonant conditions, when the feeding transmission line is longer. Extending the observation of Fig. 6 to energy figures, there are POW switching times that maintain the energy at lower levels even at longer lengths of transmission lines.

Fig. 8 illustrates the ferroresonance map determined as a function of transmission line length and POW switching. This map classifies ferroresonance results according to their steady-state condition (i.e. once the transient is over – applies only for the sustained modes, fundamental and subharmonic). However, it should be noted that transient ferroresonance phenomena present a series of risks of over-voltages and over-currents to electrical equipment, albeit for a relatively short period of time. The four different regions that are included in Fig. 9 are the sustained fundamental ferroresonance region, the subharmonic ferroresonance region, the chaotic/quasi-periodic ferroresonance region and lastly the region where the system is in no danger as ferroresonance is not present. It is interesting to note that the fundamental mode-sustained ferroresonance can occur even with short transmission lines. Lastly, it can be stated that the map reinforces the stochastic nature of the ferroresonance phenomenon.

4.2 Interaction of core losses and POW switching

The second case study presents the results obtained from the interaction of core losses and POW switching by altering these two parameters and leaving all others unchanged. Fig. 9 describes the steady-state (once the transient period ceases to exist) ferroresonant peak voltage values in p.u. and the steady-state peak current values for each of the three phases as a function of core losses and POW switching. The maximum magnitude of ferroresonant currents lies in the range of 400–500 A_{peak}. Over-voltages can go up to 2 p.u. and exist in all three phases in the case where the core losses are low.

Fig. 10 illustrates the energy transfer in the transformer under ferroresonant conditions when considering the interaction of POW switching and core losses. The energy transfer calculation has been performed at a relatively short transmission line length of 37 km. It is observed that lower core losses, show a higher energy transfer in the transformer putting it at a higher danger of overheating. POW switching determines areas with low or high energy values as is the case in Fig. 8 with voltage and current waveforms.

Fig. 11 illustrates the ferroresonance map determined as a function of core losses and POW switching. It can be seen that even though high core losses can provide a generally safer environment for a transformer in terms of ferroresonance occurring, there are certain POW switching times that can initiate sustained fundamental ferroresonance.

5 Conclusions

Utilising a validated simulation model, this paper investigated the influence of a number of system and plant parameters on ferroresonance through sensitivity studies. Specifically, the parameters under study are the transmission line length, the POW switching and core losses, and the relationship between the severity of ferroresonance in terms of peak voltage, current and energy transfer with these parameters is mapped out. Analysis of the maps shows that ferroresonance is a stochastic function, dependent on the initial conditions and circuit parameters. It is suggested that the transformer may be exposed to higher energy transfers with longer transmission lines or where the core losses are lower. Although no transformer has failed during ferroresonance activity, the impact of ferroresonance on transformers is mainly accelerated ageing and may be estimated through the energy transfer during ferroresonance. Furthermore, the main idea of the energy map in this paper is to provide a representation of the transferred energy variation in relation to the POW switching, transmission line length and core losses. The energy figures will not serve the purpose of quantifying the effect that the energy dissipation would have on the transformer; nonetheless, they become a useful indication for potential transformer damage and in addition a benchmark for further finite element studies that would calculate where the power is specifically dissipated, directly.

6 References

1 Tong, Y.K.: 'NGC experience on ferroresonance in power transformers and voltage transformers on HV transmission systems, Warning! Ferroresonance can damage your plant'. IEE colloquium, 12 November 1997

2 Araujo, A.E.A., Soudack, A.C., and Marti, J.R.: 'Ferroresonance in power systems: chaotic behaviour', *IEE Proc.*, 1993, **140**, (3), pp. 237–240

3 Charalambous, C., Wang, Z., Osborne, M., and Jarman, P.: 'Validation of a power transformer model for ferroresonance with system tests on a 400 kV circuit', I.P.ST 2007, Lyon, France, 4–7 June 2007
4 'Ferroresonance tests on Brinsworth–Thorpe marsh 400 kV circuit', National Grid Seven Year Statement. Available at: www.nationalgrid.com/sys
5 Slow Transients Task Force of the IEEE Working Group on Modeling and Analysis of Systems Transients Using Digital Programs 'Modeling and analysis guidelines for slow transients – part III: the study of ferroresonance', *IEEE Trans. Power Deliv.*, 2000, **15**, (1), pp. 255–265
6 Greene, J.D., and Gross, C.A.: 'Nonlinear modeling of transformer', *IEEE Trans. Ind. Appl.*, 1988, **24**, (3), pp. 434–438
7 Tran-Quoc, T., and Pierrat, L.: 'An efficient non linear transformer model and its application to ferroresonance study', *IEEE Trans. Magn.*, 1995, **31**, (3), pp. 2060–2063
8 Al Zahawi, B.A.T., Emin, Z., and Tong, Y.K.: 'Chaos in Ferroresonance wound voltage transformers:effect of core losses and universal circuit behaviour', *IEE Proc., Sci. Meas. Technol.*, 1998, **145**, (1), pp. 39–43
9 Al-Anbarri, K., Ramanujam, R., Saravanaselvan, R., and Kuppusamy, K.: 'Effect of iron core loss nonlinearity on chaotic ferroresonance in power transformers', *Electr. Power Syst. Res.*, 2003, **65**, (1), pp. 1–12
10 Pedra, J., Sainz, L., Corcoles, F., Lopez, R., and Salichs, M.: 'PSPICE computer model of a nonlinear three-phase three-legged transformer', *IEEE Trans. Power Deliv.*, 2004, **19**, (1), pp. 200–207
11 Mork, B.A., Gonzalez, F., Ishchenko, D., Stuehm, D.L., and Mitra, J.: 'Hybrid transformer model for transient simulation – part 1: development and parameters', *IEEE Trans. Power Deliv.*, (2007, **22**, (1), pp. 248–255
12 'ATP rule book and theory book', Can/AM EMTP User Group, Portland, OR, USA, 1997
13 British Electricity International: 'Modern power station practice', EHV Transmission (Pergamon Press), vol. K
14 Marti, J.R., and Soudack, A.C.: 'Ferroresonance in power systems: fundamental solutions', *IEEE Proc.*, 1991, **138**, (4), pp. 321–329
15 Mork, B.A.: 'Five-legged wound-core transformer model: derivation, parameters, implementation, and evaluation', *IEEE Trans. Power Deliv.*, 1999, **14**, (4), pp. 1519–1526
16 Emin, Z., Al Zahawi, B.A.T., Auckland, D.W., and Tong, Y.K.: 'Ferroresonance in electromagnetic voltage transformers: a study based on nonlinear dynamics', *IEEE Proc., Gener. Transm. Distrib.*, 1997, **144**, (4), pp. 383–388
17 Martinez, J.A., and Mork, B.A.: 'Transformer modeling for low- and mid-frequency transients – a review', *IEEE Trans Power Deliv.*, 2005, **20**, (2), pp. 1625–1632
18 Wang, Z.D.: 'Location of partial discharges in power transformers', PhD thesis, UMIST, Manchester, UK, 1999
19 Cunningham, W.J.: 'Introduction to nonlinear analysis' (McGraw-Hill, New York, 1958), pp. 157–168